

Effect of Short-Duration Low-Magnitude Cyclic Loading Versus Immobilization on Tendon-Bone Healing After ACL Reconstruction in a Rat Model

By Robert H. Brophy, MD, David Kovacevic, MD, Carl W. Imhauser, PhD, Mark Stasiak, MSE, Asheesh Bedi, MD, Alice J.S. Fox, MD, Xiang-Hua Deng, MD, and Scott A. Rodeo, MD

Investigation performed at the Laboratory for Soft Tissue Research, Hospital for Special Surgery, New York, NY

Background: Successful anterior cruciate ligament reconstruction with use of soft-tissue grafts requires healing between tendon and bone. Little is known about the effect of mechanical load on the cellular and molecular cascade of tendon-to-bone healing. Understanding these mechanical influences has critical implications for postoperative rehabilitation following anterior cruciate ligament reconstruction. The purpose of this study was to test the hypothesis that, compared with perioperative immobilization, short-duration low-magnitude cyclic axial loading would result in impaired tendon-to-bone healing after anterior cruciate ligament reconstruction in a rat model.

Methods: Fifty-two male Sprague-Dawley rats underwent anterior cruciate ligament reconstruction with use of a flexor digitorum longus autograft. The patellar tendon, capsule, and ligamentous structures were circumferentially released, and an external fixator parallel to the anterior cruciate ligament graft was placed across the knee. Mechanical loading, consisting of cyclic displacement of the femur and tibia constrained to axial translation parallel to the graft, was applied daily. The rats were randomly assigned to immobilization or daily loading, for fourteen or twenty-eight days. Biomechanical, micro-computed tomographic, and histomorphometric analysis was performed on the bone-tendon-bone complexes.

Results: The load measured across the knees during cyclic displacement increased over time ($p < 0.05$). Load-to-failure testing of the isolated femur-anterior cruciate ligament graft-tibia specimens revealed no significant differences between groups at two or four weeks. By two weeks postoperatively, a greater number of ED1+ inflammatory macrophages (phagocytic cells involved in the initial injury response) were seen at the tendon-bone interface after loading in the cyclically loaded group than in the immobilized group ($p = 0.01$). Compared with the baseline values, the number of trabeculae was significantly lower after loading for four weeks ($p = 0.02$).

Conclusions: Short-duration low-magnitude cyclic axial loading of the anterior cruciate ligament graft in the postoperative period is not detrimental to the strength of the healing tendon-bone interface but appears to be associated with greater inflammation and less bone formation in the tunnel in this rat model.

Clinical Relevance: Further investigation of varied timing and magnitude of graft-loading may help guide postoperative rehabilitation protocols following anterior cruciate ligament reconstruction with soft-tissue grafts.

Tendon-to-bone healing is critical to the ultimate success of several orthopaedic procedures. The native tendon or ligament insertion to bone is a highly specialized and organized tissue that functions to transmit complex mechanical loads from soft tissue to bone. The insertion site contains four distinct types of tissue: tendon, unmineralized fibrocartilage, mineralized fibrocartilage, and bone¹. Previous animal studies

have shown that healing between bone and a tendon graft occurs by formation of fibrovascular scar tissue and ingrowth of new bone into the graft^{2,3}. The structure and composition of the native enthesis are not recapitulated during healing, resulting in a mechanically and structurally inferior interface^{4,5}.

Despite strong evidence that mechanical stimulation affects the healing of both bone and soft tissue, there is a paucity

Disclosure: In support of their research for or preparation of this work, one or more of the authors received, in any one year, outside funding or grants in excess of \$10,000 from the National Institutes of Health (Grant R01 AR053689-01A1). Neither they nor a member of their immediate families received payments or other benefits or a commitment or agreement to provide such benefits from a commercial entity.

of literature examining the effect of mechanical load on healing at the tendon-bone interface. Thomopoulos et al.⁶ found that early exercise impaired rotator cuff tendon-healing in a rat model. Better healing was observed in rats that were immobilized postoperatively. In a rabbit model of anterior cruciate ligament (ACL) reconstruction, Sakai et al.⁷ found improved healing and graft attachment strength with postoperative immobilization of the limb postoperatively compared with the healing and strength seen in animals that were allowed normal cage activity postoperatively. In a canine flexor tendon-to-bone injury and repair model, repaired tendons with the proximal end of the tendon intact (resulting in load on the tendon) healed with greater stiffness than did repaired tendons with the proximal end of the tendon cut.⁸ In that canine study, paws in both groups were casted and subjected to daily passive motion. An important limitation of these studies is that the mechanical stimulation of the healing tendon-bone interface was neither quantified nor controlled.

We developed a novel rat model of ACL reconstruction using an external fixator that allows controlled postoperative axial loads to be cyclically applied to the healing tendon-bone interface. In this study, we studied the effect of rigid postoperative immobilization as compared with immediate, short-duration low-magnitude cyclic axial loading after ACL reconstruction. Our overall hypothesis was that immediate loading of the healing ACL graft would impair early tendon-bone healing in comparison with the healing seen with immobilization. Our specific hypotheses were that immediate low-magnitude loading of the healing ACL graft would result in (1) more inflammation, neoangiogenesis, and osteoclast accumulation at the healing interface; (2) less new bone formation at the healing tendon-bone interface; and (3) reduced graft attachment strength and stiffness.

Materials and Methods

After obtaining Institutional Animal Care and Use Committee approval and optimizing the surgical technique on cadaveric animals, seventy-two male Sprague-Dawley rats (weight, 250 to 350 g) underwent ACL reconstruction with use of a flexor digitorum longus autograft. The rats were randomly assigned to either of two postoperative regimens: immobilization or daily cyclic loading, for fourteen or twenty-eight days. At the end of the study period, the animals were killed for biomechanical testing, micro-computed tomography (micro-CT), histomorphometric analysis, and immunohistochemical analysis.

Surgical Technique

The surgical procedure was performed on the right lower limb of an anesthetized rat. After preparing the animal for surgery, a flexor digitorum longus autograft was harvested from the ipsilateral limb. A medial parapatellar arthrotomy was performed. The patellar tendon, collateral ligaments, anterior and posterior cruciate ligaments, and anterior capsule were all sectioned. The posterior aspect of the capsule was bluntly elevated and was detached from the posterior aspect of the tibia but not divided.

Free of restraint (except for the posterior musculature and neurovascular bundle), the tibiofemoral joint was flexed to approximately 60°. A Keith needle (1.2 mm in diameter) was used to drill the tibial and femoral tunnels with use of a trans-tibial technique, with care taken to capture the tibial and femoral ACL footprints. The Keith needle was left in place across the knee and was used to guide parallel alignment of the external fixator. The external fixator was aligned with use of custom-fabricated jigs that were positioned on the Keith needle, allowing the external fixator bar to be secured parallel to the bone tunnels and ACL graft. Custom-designed connectors were fixed to the threaded pins and the fixation bar and could be interfaced to the loading device for daily cyclic loading.

To place the external fixator, two parallel 0.9-mm threaded pins were placed centrally into the distal part of the femur from the lateral side through separate stab incisions spaced approximately 5 mm apart. The external fixator was then secured to the femoral pins and used to guide the insertion of two 0.9-mm threaded pins (1600-635T Kirschner wire; MicroAire Surgical Instruments, Charlottesville, Virginia) centrally into the proximal part of the tibia from the lateral side. The entire external fixator was then tightly secured to maintain the fixator bar in a position parallel to the Keith needle and, eventually, to the ACL graft (Fig. 1). The Keith needle was then used to shuttle the flexor digitorum longus autograft tendon through the bone tunnels, replacing the native ACL. As the tendon graft was manually tensioned via 3-0 Ethibond stay sutures (Ethicon, Somerville, New Jersey) in each end of the graft, it was secured to the periosteum and surrounding fascia of the distal part of the femur and proximal part of the tibia with 3-0 Ethibond suture. The length of the graft was measured with use of calipers from the extra-articular entrance of the tibial tunnel to the exit of the femoral tunnel, and the wound was closed in a standard layered fashion.

Loading Protocol

A computer-controlled loading device that could be secured to the connectors of the external fixator was designed and fabricated. After the connectors were secured to the loading device, the fixation bar was removed (Fig. 2). A computer-controlled stepper motor (Model 18503; Oriel, Stratford, Connecticut) directed the loading device to apply axial distraction or compression to the tibiofemoral joint, parallel to the graft tunnels, thus enabling the application of axial elongation to the graft. The linear constraint on the motion is provided by a linear bearing consisting of two roller bearing blocks on a rigid linear rail. One block is oscillated by the stepper motor, while the other is held stationary by the load cell. The linear rail carries transverse loads, which would otherwise be transmitted to the ACL bone-graft-bone construct. Displacement is measured with use of a linear variable differential transducer (Schaevitz LBB315 PA-100; Measurement Specialties, Hampton, Virginia), and the load transmitted across the knee joint is measured by a load cell (MDB-5; Transducer Techniques, Temecula, California). The loading device records the resulting load-displacement curves.

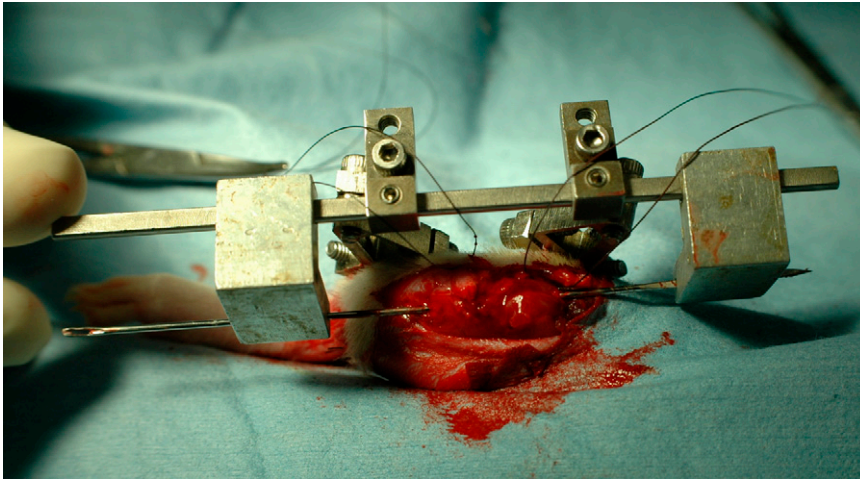


Fig. 1
Example of mounted external fixator on specimen with Keith needle in place.

The loading protocol was performed daily in the treatment group for fifty cycles. After induction of 2% isoflurane inhalation anesthesia, the external fixator was connected to the loading device. The level of graft elongation was chosen on the basis of previous studies that reported 2% to 5% elongation of both the native ACL and ACL grafts in the human knee during light rehabilitation exercises such as pedaling on a stationary bicycle⁹⁻¹¹. Preliminary cadaveric studies confirmed mean normalized graft elongation of 2.2% with use of the loading protocol outlined below.

The local distraction of the reconstructed knee joint during the loading protocol was confirmed with a preliminary analysis of nine rat cadaver specimens. Knee distraction was measured with use of a motion analysis system (ProReflex MCU; Qualisys, Gothenburg, Sweden) with an accuracy of 50 μm .

A reflective marker was placed at the graft tunnel exits of both the femur and the tibia. As the distraction device pulled the knee joint apart using the experimental protocol, the cameras tracked the three-dimensional spatial position of the two markers. Knee distraction was calculated as the change in the distance between markers, comparing the unloaded knee to the knee at maximal load. The slack in the reconstructed ACL graft was also incorporated as part of the loading protocol because displacement control was used to mechanically stimulate the graft. Slack was defined as the distance required for the isolated graft to begin taking load. The mean measured initial slack length (and standard deviation) was 0.55 ± 0.23 mm, while the mean knee distraction was 0.88 ± 0.33 mm. The mean total joint distraction was 0.33 mm, which equated with a mean graft elongation of 2.2% when normalized to the average graft length of 15 mm.



Fig. 2
Example of animal connected to loading device.

We first applied compression of 1.96 N (200 g) across the joint to establish a consistent starting point. The joint was then distracted at 0.24 mm/sec until the tibia and femur reached the total distraction distance (as defined by the evaluative experiments described above) and was then returned to the neutral position for a total of fifty cycles. The resulting load-displacement curve was recorded for each cycle. The entire loading protocol required approximately twenty minutes of anesthesia time each day, which was well tolerated by all animals. After the loading protocol was completed, the fixation bar was reattached to the external fixator and the animal was returned to its cage where it awakened from anesthesia and resumed normal cage activity.

Animals allocated to the immobilization group were allowed normal cage activity with the external fixator in place, and they did not undergo any controlled loading throughout the study period. The anesthetized, immobilized animals were connected to the computer-controlled loading device immediately before they were killed, however, to obtain a one-time load-displacement response for comparison with the loading groups. Immediately after the animals were killed, the specimens from the daily loading groups were stripped of all soft tissue except for the ACL graft and underwent one loading session, consisting of twenty cycles, to determine the load in the isolated bone-tendon-bone construct.

Histological Analysis

Three specimens were randomly assigned to histological analysis for each treatment group and time point. After the animal was killed, the intra-articular portion of the graft was divided to generate separate tibial and femoral specimens. The specimens were then fixed and decalcified with use of standard techniques. The tissues were embedded in paraffin, and 5- μ m-thick sections were cut in the coronal plane for the tibia and in the sagittal plane for the femur. Serial sections were collected for routine histological analysis with use of hematoxylin and eosin, safranin-O, and picosirius red staining.

We optimized the staining conditions (i.e., appropriate antibody dilutions and antigen retrieval techniques) for all of the antibodies used in the immunohistochemical analyses¹². Serial sections were treated with 3% H₂O₂ to quench endogenous peroxidase activity, and nonspecific antibody binding was blocked with 5% goat serum. Each primary antibody was applied to separate serial sections for sixty minutes at 37°C. Bound antibodies were visualized with use of a goat avidin-biotin peroxidase system with 3,3'-diaminobenzidine (DAB; DAKO, Carpinteria, California) as a substrate. The following antibodies were used to localize hematopoietic lineage cells: rabbit anti-rat neutrophil (PMN) (Accurate Chemicals, Westbury, New York), mouse anti-rat ED1-macrophage (ED1 antigen is a lysosomal glycoprotein expressed only by a subpopulation of macrophages and monocytes), and mouse anti-rat ED2-macrophage (ED2 antigen is a membrane glycoprotein found only on mature tissue macrophages) (Serotec, Raleigh, North Carolina). Osteoclast activity was evaluated by staining for tartrate-resistant acid phosphatase (TRAP; Zymed, San Francisco, California). For the assessment of osteoblast activity,

Type-I procollagen (Santa Cruz Biotechnology, Santa Cruz, California) was localized as an indicator of collagen synthesis. Proliferating blood vessels were localized with use of rabbit anti-human factor VIII (DAKO). The sections were counterstained with Mayer's hematoxylin. Negative controls were processed in an identical manner except for incubation with bovine serum albumin rather than the primary antibody.

Analysis of Histological Data

The histological sections were examined with use of light microscopy (Eclipse E800; Nikon, Melville, New York), and digital images of the stained tissue sections were made with use of a SPOT RT camera (Diagnostic Instruments, Sterling Heights, Michigan). The number of positively-stained cells was counted in thirty randomly-selected high-power ($\times 40$ magnification) microscopic fields distributed along the bone tunnel. These measurements were limited to the tibial tunnel since there was variability in the quality of the femoral tunnel sections due to the small size of the bone. Two observers (D.K. and S.A.R.) who were experienced with immunohistochemical analyses independently counted positively-stained cells on the ED1 and ED2-stained slides. There was >95% agreement between the observers. On the basis of this analysis, further sections were all scored by one observer. Random data checking was performed for the other specific immunohistochemical analyses to confirm that this level of agreement was maintained throughout the histological analysis. Inflammation was quantified by counting the numbers of macrophages and polymorphonuclear cells. The number of positively stained cells for all other markers was also counted at the tendon-bone interface.

Micro-CT Analysis

Trabecular architecture, bone formation, and bone remodeling along the tendon-bone interface were assessed with use of micro-CT (MS-8 Small Specimen Scanner; Enhanced Vision Systems, London, Ontario, Canada). Four specimens in each treatment group underwent micro-CT analysis at two and four weeks postoperatively. Time-zero analysis was also performed on three specimens to provide a baseline reference for comparison with the data from later time points. The tibial and femoral tunnels were scanned and reconstructed at 22.5- μ m isotropic resolution. Each sample was placed in the holder surrounded by saline solution and scanned at 80 V and 80 mA. The scans included a phantom containing air, saline solution, and a bone reference material for calibration of Hounsfield units to tissue mineral density. A global threshold, based on the histogram of CT attenuation values derived from the Otsu discriminant¹³, was used for each specimen to distinguish bone voxels in the images.

After thresholding, six outcome measures were evaluated: bone volume (mm³), tissue mineral content (mg), tissue mineral density (mg/mL), trabecular thickness (μ m), trabecular number, and trabecular spacing (μ m). The total bone mineral content, bone volume fraction (bone volume divided by total volume), and mineral distribution were calculated for a cylindrical volume of interest, with a diameter of 2.2 mm, cen-

TABLE I Inflammatory Cell Histology Data*

Marker and Time Point	Cells per High-Power Field	
	Immobilized Groups	Loaded Groups
ED1+ cells		
2 weeks		
Mean	2.4 ^a	3.0 ^{a,b}
Median	2.0	3.0
Standard deviation	1.5	1.5
4 weeks		
Mean	2.6	1.9 ^b
Median	3.0	2.0
Standard deviation	1.5	1.4
ED2+ cells		
2 weeks		
Mean	1.6	1.2
Median	1.0	1.0
Standard deviation	1.8	1.3
4 weeks		
Mean	0.8	1.4
Median	0.0	1.0
Standard deviation	1.3	1.3
Polymorphonuclear cells		
2 weeks		
Mean	0.6	0.3
Median	0.0	0.0
Standard deviation	1.0	0.6
4 weeks		
Mean	0.3	0.2
Median	0.0	0.0
Standard deviation	0.8	0.7

*The letters a and b identify the two data points being compared in each case, with a indicating a p value of 0.01, and b indicating a p value of 0.03.

tered along the graft tunnel for the entire length of each graft. The bone volume is the total number of thresholded bone voxels within the total volume of interest. The mineral distribution along the graft was determined from the computed tomography value for each voxel in the micro-CT scan. An SB3 standard (1100 g of hydroxyapatite/cm³) was used to calibrate bone mineral density in each scan.

Biomechanical Testing

Six rats in each group were assigned to biomechanical testing. At the two or four-week interval, rats were killed and the femur-graft-tibia construct was carefully harvested and stored at -80°C. Prior to testing, the specimens were thawed and all soft tissue was dissected, preserving only the graft crossing the knee. The tibia and femur were potted in cement (Bondo; 3M Bondo, Atlanta, Georgia) to ensure secure fixation. Specimens were

mounted on a custom-designed tensile testing apparatus with a specially designed jig that allowed alignment of the axis of distraction parallel to the long axis of the graft. Saline-solution spray was used to maintain specimen hydration throughout testing. The specimens were first preconditioned for five cycles by submitting them to a tension load between 0 and 0.2 N, and then they were loaded in tension to failure at a rate of 10 mm/min (167 μm/sec). The ultimate load (N) was obtained from the recorded load-deformation curve, and stiffness (N/mm) was calculated from the linear portion of this curve with use of Microsoft Office Excel 2002 (Microsoft, Redmond, Washington). The site of graft failure (graft midsubstance, femoral tunnel, or tibial tunnel) was also recorded.

Statistical Analysis

A custom-designed program in MATLAB 6.1 (The MathWorks, Natick, Massachusetts) was used to record the load at maximum displacement from cycles 21 to 30 of the daily loading treatment for each animal in the two-week or four-week loading groups. The mean load at maximum displacement from cycles 21 to 30 was calculated for up to twenty-eight days after surgery. One-way analysis of variance with repeated measures was used to assess for significant changes in the mean load at maximum displacement for each animal over the postoperative course. A Student t test was used to compare the mean load between the two-week and four-week daily loading groups at various time points after surgery and after isolating the graft on the day that the animal was killed. On the day on which the animals were to be killed, the two-week and four-week immobilization groups underwent one loading session, consisting of fifty cycles, to allow comparison of these peak loads to those of the daily loading groups. Statistical analysis of graft structural properties was performed with use of two-way analysis of variance. Differences in outcomes between the times at which the animal was killed and between loading regimens were considered in the two-way analysis of variance. Analysis of the histological data

TABLE II Angiogenesis Histology Data*

Factor VIII	Cells per High-Power Field	
	Immobilized Groups	Loaded Groups
2 weeks		
Mean	0.8 ^a	1.6 ^{a,b}
Median	0.0	2.0
Standard deviation	1.0	1.1
4 weeks		
Mean	1.1	0.7 ^b
Median	0.0	0.0
Standard deviation	1.4	0.9

*The letters a and b identify the two data points being compared in each case, with both a and b indicating a p value of 0.08.

TABLE III Bone Homeostasis Histology Data*

Marker and Time Point	Cells per High-Power Field	
	Immobilized Groups	Loaded Groups
TRAP staining		
2 weeks		
Mean	1.4 ^a	1.0
Median	1.0	1.0
Standard deviation	1.2	1.0
4 weeks		
Mean	0.7 ^a	1.2
Median	0.0	1.0
Standard deviation	1.0	0.9
Procollagen staining		
2 weeks		
Mean	1.7	3.2
Median	2.0	3.0
Standard deviation	1.2	1.7
4 weeks		
Mean	2.6	2.0
Median	3.0	2.0
Standard deviation	1.7	1.6

*The letter a identifies the two data points being compared, and indicates a p value of 0.07. TRAP = tartrate-resistant acid phosphatase.

was performed with use of a repeated-measures analysis of variance with a simple random sampling taken for each of the markers. Post-hoc tests were conducted with use of the Holm-Sidak

method. All statistical analysis was performed with use of Systat Software (Chicago, Illinois) or SAS 9.1 for Windows (SAS Institute, Cary, North Carolina), and significance was set at $p < 0.05$.

Source of Funding

This study was funded by National Institutes of Health Grant R01 AR053689-01A1. There was no other source of funding for this study.

Results

Histology

An example of a negative control slide is shown in Figure 3.

Inflammatory Cells

Data on inflammatory cells are summarized in Table I. ED1+ inflammatory macrophages were abundant regardless of group or time point (Fig. 4). There were significantly more ED1+ macrophages in the loaded group at two weeks (3.0 ± 1.5 cells per high-power field) than there were in the immobilized group (2.4 ± 1.5 cells per high-power field) ($p = 0.01$) (Table I). In the immobilized group, the number of ED1+ macrophages remained constant over time. In the loaded group, the number of ED1+ macrophages decreased to 1.9 ± 1.4 cells per high-power field at four weeks ($p = 0.03$ for two-week versus four-week numbers). There was no significant difference between the loaded or immobilized specimens at four weeks. Concentrations of ED2+ resident macrophages demonstrated no significant differences between groups at either time point and no significant changes over time. Very few neutrophils were seen, with no appreciable differences regardless of the observation period or loading protocol.

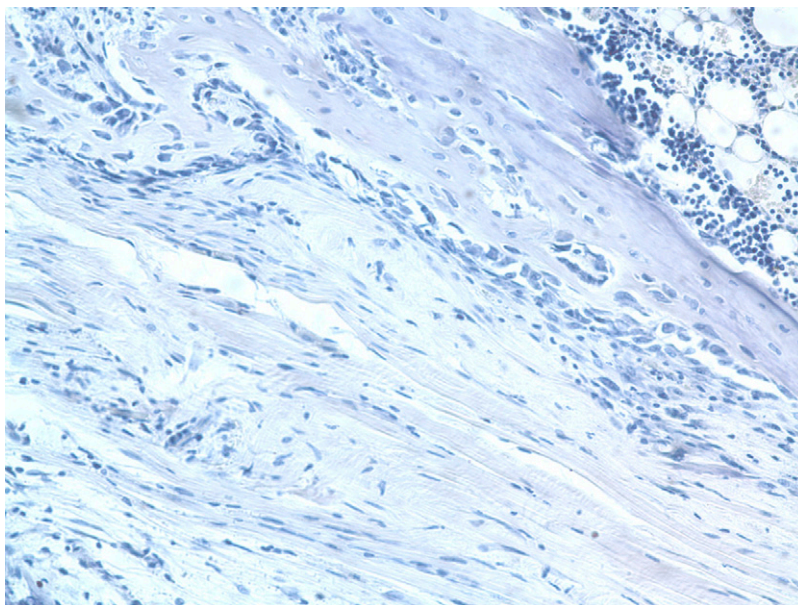


Fig. 3

Example of negative control histology (mouse anti-rat ED1- microphage stain; original magnification, $\times 20$).

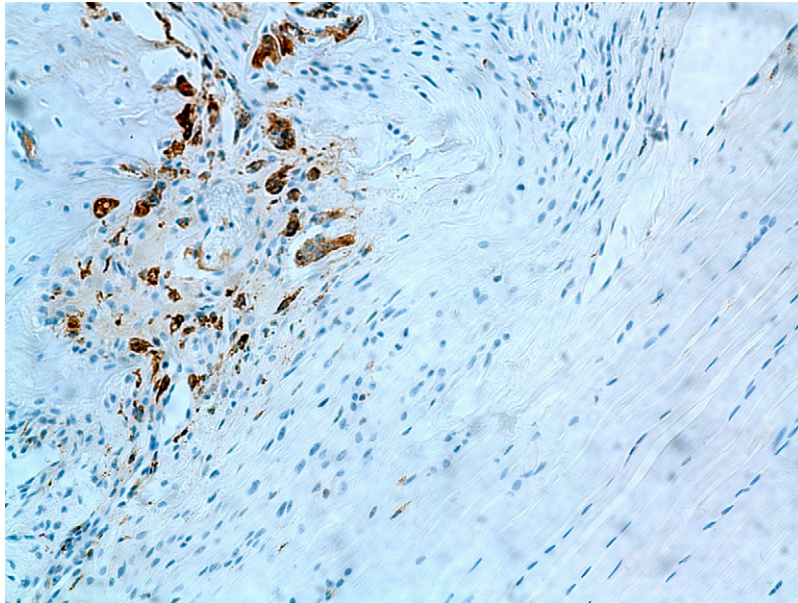


Fig. 4
ED1 staining (mouse anti-rat ED1-macrophage stain) showing inflammatory macrophages in the tissue of a rat from the immobilized group killed at two weeks (original magnification, $\times 20$).

Angiogenesis

Factor-VIII staining (Fig. 5) showed no significant difference in the number of endothelial cells localized to the tendon-bone interface in the loaded group as compared with the immobilization group at two weeks postoperatively ($p = 0.08$) (Table II). The number of endothelial cells remained constant in the immobilization group from two to four weeks, whereas the

loaded group exhibited half as many endothelial cells in the tibial tunnel at four weeks as it did at two weeks ($p = 0.08$).

Osteoclasts and Osteoblasts

Histology data related to bone homeostasis are summarized in Table III. In the immobilization group, there was no significant difference in tartrate-resistant acid phosphatase staining over

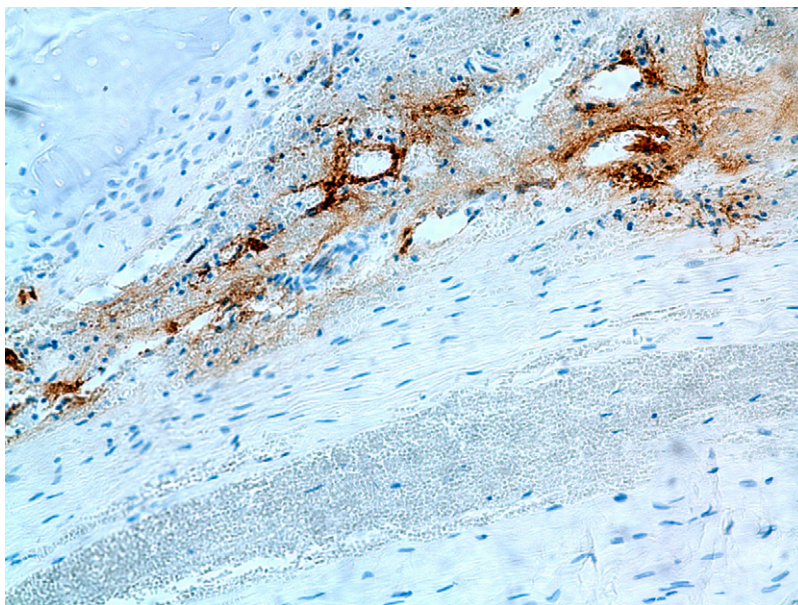


Fig. 5
Factor VIII staining (rabbit anti-human factor VIII, DAKO) showing endothelial cells in the tissue of a rat from the immobilized group killed at four weeks (original magnification, $\times 20$).

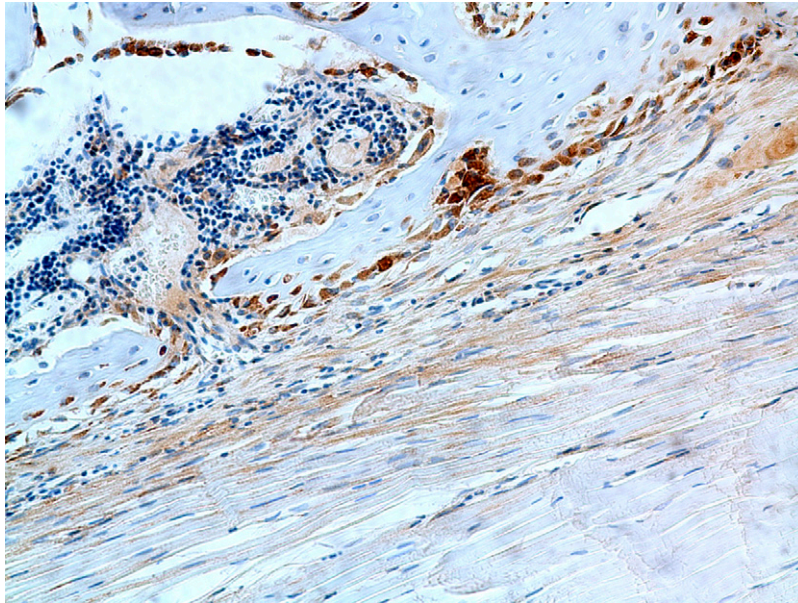


Fig. 6
Procollagen staining (Santa Cruz Biotechnology) revealing collagen synthesis in the tissue of a rat from the immobilized group killed at four weeks (original magnification, $\times 20$).

time (1.4 ± 1.2 cells per high-power field versus 0.7 ± 1.0 cells per high-power field, $p = 0.07$). The number of osteoclasts remained constant over time in the loaded group. There were no significant differences between the two treatment groups at either time point. There were no differences in procollagen staining between the two treatment groups at either time point (Fig. 6).

Micro-CT

The micro-CT data are summarized in Table IV. The number of trabeculae was significantly lower after loading for four weeks

(Figs. 7-A and 7-B) compared with the number at baseline ($p = 0.02$). There were no other significant differences when the number was compared over time or by loading protocol.

Biomechanical Testing

Daily Cyclic Loading of the Intact Knee Joint

In rats that underwent daily loading, the mean load measured across the knee increased from 5.7 ± 2.3 N on postoperative day 1 to a final value of 9.8 ± 2.4 N by two weeks ($p = 0.04$), and from 4.1 ± 0.9 N on postoperative day 1 to a final value of 9.4 ± 4.0 N by four weeks ($p = 0.03$) (Fig. 8). For all groups,

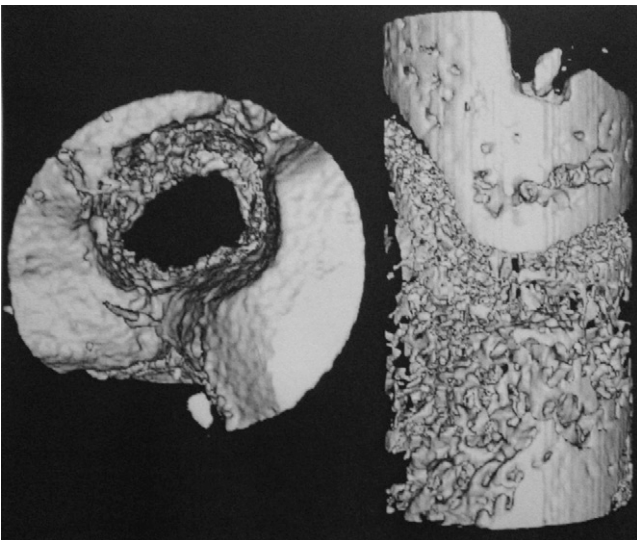


Fig. 7-A

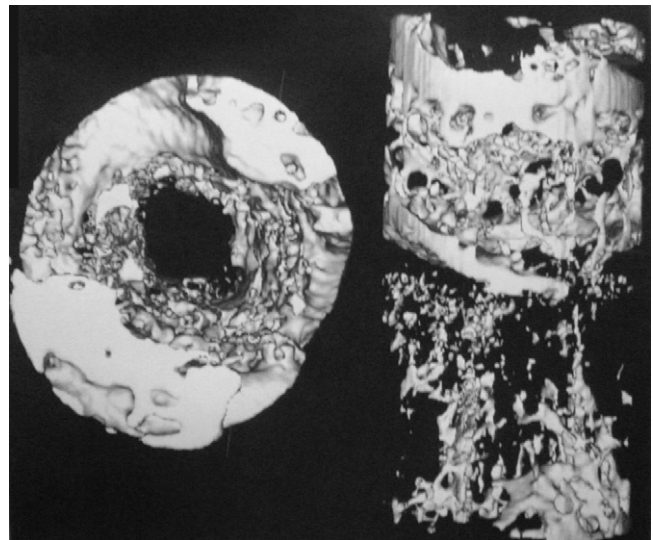


Fig. 7-B

Micro-CT showing the tibial tunnel of rats killed at four weeks from the immobilized group (Fig. 7-A) and the loaded group (Fig. 7-B).

TABLE IV Micro-Computed Tomography Data*

	Time Zero (N = 3)	2 Weeks		4 Weeks	
		Immobilized Group (N = 4)	Loaded Group (N = 4)	Immobilized Group (N = 4)	Loaded Group (N = 4)
Bone volume (mm ³)	0.82 ± 0.04	0.85 ± 0.19	0.89 ± 0.30 ^a	0.88 ± 0.28 ^b	0.61 ± 0.09 ^{a,b}
Total mineral content (mg)	0.45 ± 0.03	0.48 ± 0.12	0.49 ± 0.15	0.49 ± 0.17	0.37 ± 0.08
Total mineral density (mg/mL)	543 ± 25	542 ± 32	536 ± 40	534 ± 40	575 ± 39
Trabecular thickness (μm)	61.6 ± 2.6	69.8 ± 13.1	67.5 ± 13.2	66 ± 11.3	58.2 ± 2.66
Trabecular number	3.71 ± 0.28 ^c	2.94 ± 0.33	2.94 ± 0.33	2.75 ± 1.02	2.61 ± 0.33 ^c
Trabecular spacing (μm)	246 ± 30 ^d	280 ± 45	297 ± 68	368 ± 188	375 ± 51 ^d

*The values are given as the mean and standard deviation. The letters a, b, c, and d identify the two data points being compared in each case; a indicates a p value of 0.07, b indicates a p value of 0.08, c indicates a p value of 0.02, and d indicates a p value of 0.09.

loads measured on and after day 10 were significantly greater than those measured on and before day 5 ($p = 0.01$). Furthermore, loads achieved on and after day 12 were significantly greater than those measured on and before day 7 ($p = 0.01$). The mean load measured across the knee at the time of death was 10.7 ± 2.9 N in the fourteen-day immobilized group and 10.9 ± 4.6 N in the twenty-eight-day immobilized group.

The load measured across the isolated bone-tendon-bone construct in the fourteen-day loaded group (0.8 ± 0.9 N) was less than that in the twenty-eight-day loaded group ($2.0 \pm$

1.5 N) ($p = 0.005$) after removing all soft tissues except the graft and repeating the loading protocol.

Biomechanical Failure Testing of the Isolated Femur-Graft-Tibia Construct

At the two-week time point, the mean stiffness was 3.8 ± 1.4 N/mm in the immobilized group and 4.1 ± 1.6 N/mm in the loaded group (Fig. 9). At four weeks, the stiffness in the immobilized group (6.4 ± 2.9 N/mm) was significantly greater than that at two weeks ($p = 0.03$), whereas the stiffness in the loaded group at four weeks (5.7 ± 1.3 N/mm) was not signif-

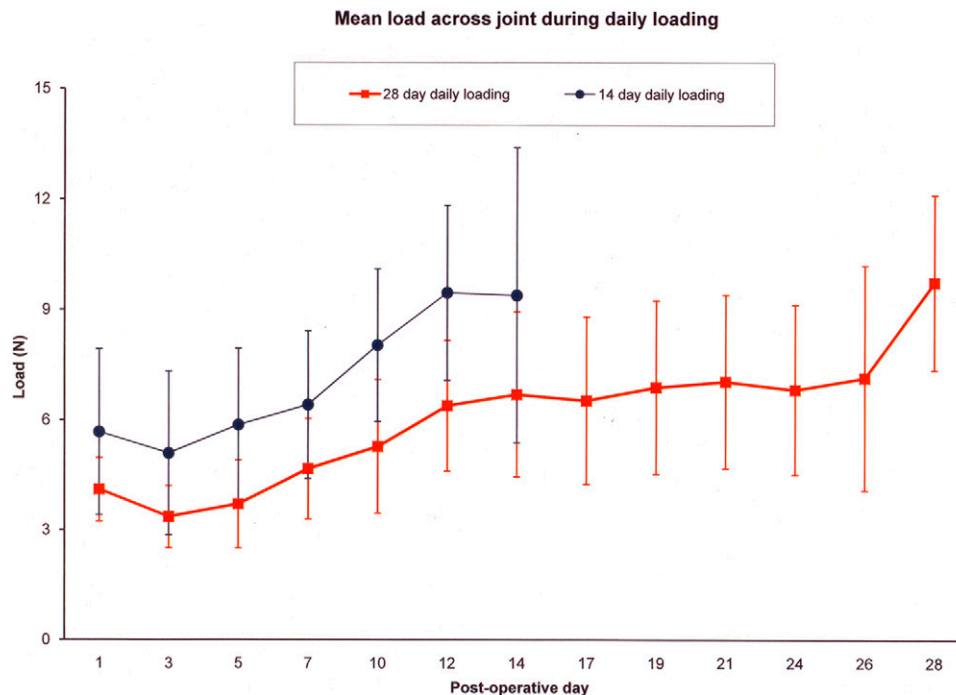


Fig. 8

Graph showing the mean daily loading curve (and standard deviation) of the rats that underwent daily loading for two weeks or four weeks.

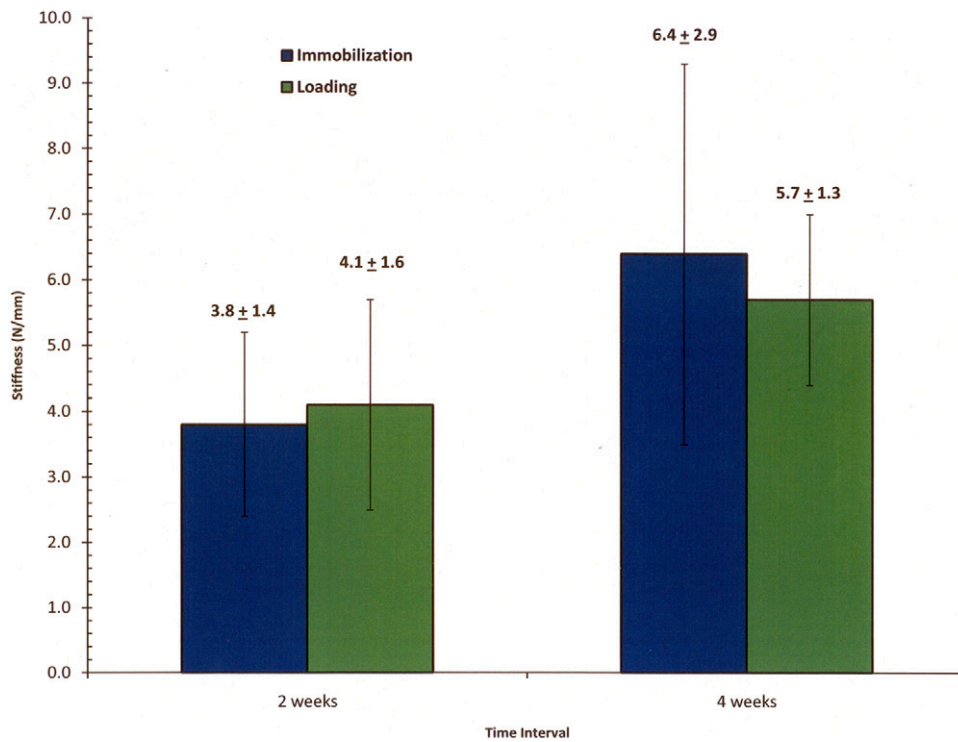


Fig. 9
Graph showing the mean stiffness data (and standard deviation) from isolated bone-tendon-bone specimens.

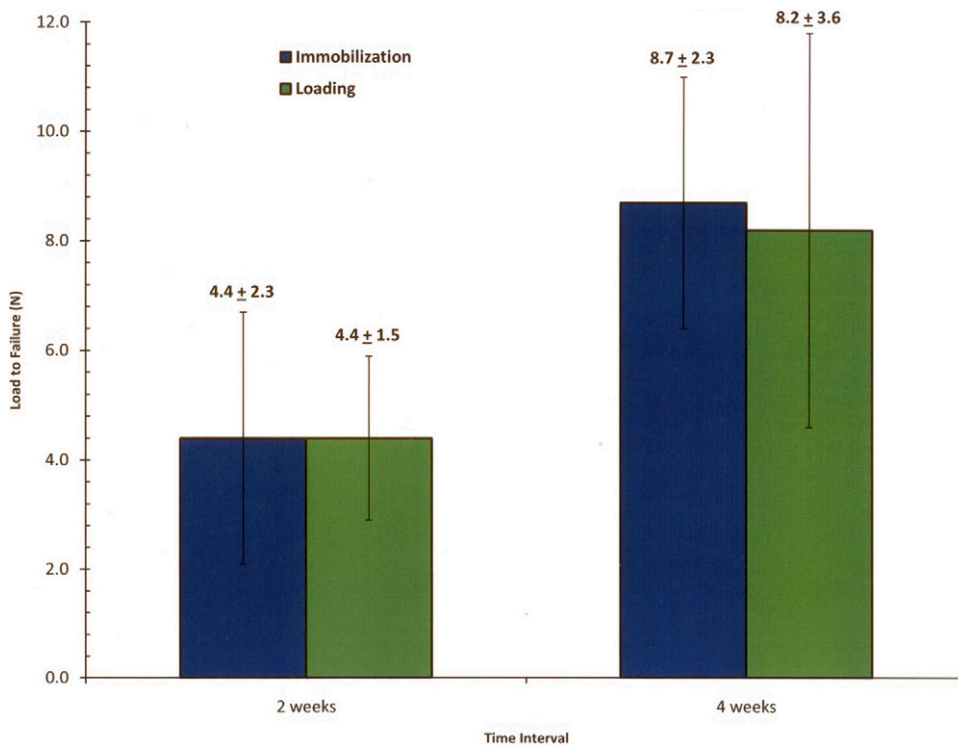


Fig. 10
Graph showing the mean load-to-failure data (and standard deviation) from isolated bone-tendon-bone specimens.

icantly different from that at two weeks. At both the two and four-week time points, there was no significant difference in stiffness between the loaded and immobilized groups.

Load to failure demonstrated similar trends with regard to stiffness (Fig. 10). At two weeks, the mean ultimate load to failure of the bone-graft-bone complexes for both immobilized and loaded groups was similar (immobilized group, 4.4 ± 2.3 N; loaded group, 4.4 ± 1.5 N). At four weeks, the mean load-to-failure for both groups almost doubled (immobilized group, 8.7 ± 2.3 N; loaded group, 8.2 ± 3.6 N), demonstrating significant increases in both groups over time (immobilized group, $p = 0.009$; loaded group, $p = 0.02$). However, there was no significant difference in load to failure between the immobilized and loaded groups at either the two or four-week time points. The tendon pulled out of either the tibial or femoral tunnel in twenty-three of the twenty-four tested specimens. One specimen from the four-week immobilization group failed through mid-substance rupture of the graft.

Discussion

We used a novel in vivo rat model to evaluate the effect of immediate low levels of cyclic axial loading for a short duration on the healing tendon-bone interface following ACL reconstruction. Our overall hypothesis was that, compared with immobilization, immediate loading of the healing ACL graft would impair tendon-bone healing. Mechanical stimulation was applied via a displacement-control loading protocol that made use of a novel cyclic distraction system, providing a unique opportunity to evaluate both the timing and magnitude of applied load on tendon-bone healing. The results provide a baseline for future studies looking at variables such as when to initiate the application of strain after surgery as well as the magnitude and duration of strain. These experiments may ultimately provide critical information that may help guide rehabilitation protocols after ACL reconstruction.

Our results partly supported our first hypothesis that immediate repetitive low-level axial loading of the ACL reconstruction would increase the accumulation of inflammatory cells at the healing interface. Immediate loading resulted in increased macrophage accumulation at two weeks. However, we did not find significant differences in blood vessels or histological indices of either bone formation or bone resorption between the groups. The discrepancy between histological findings and the micro-CT findings may be due to the relatively small area that can be examined histologically, which is in contrast to micro-CT analysis, which allowed us to examine the whole length of the bone tunnel. Our study is limited by the small number of samples for histology.

Prior studies have demonstrated the importance of macrophages at the healing tendon-bone interface^{12,14}. ED1+ macrophages are phagocytic cells that remove debris^{15,16} and appear in high concentrations early after injury¹⁷. In contrast, ED2+ macrophages are derived from local cells, accumulate later in the healing cycle^{15,18}, and appear to have an anabolic role in tendon repair¹⁸. The results of the present study indicate that ED1+ macrophages appear to be more sensitive to mechanical load

than ED2+ macrophages are. There were significantly more ED1+ macrophages in the loaded group at two weeks than there were in the immobilized group, which was followed by a decrease in the number of ED1+ macrophages over time in the loaded specimens but not in the immobilized group. Few ED2+ macrophages were seen, and the number of ED2+ macrophages did not change significantly over time in either group.

There is a distinct temporal sequence of macrophage accumulation in tendon-healing. In a prior study that localized ED1+ and ED2+ macrophages at the tendon-bone interface, macrophages first appeared at the tendon-bone interface and then migrated progressively into the tendon¹². In that study, the ED1+ macrophages were the most common cell type, appearing as early as four days after surgery and accounting for 50% of cells present at this time point. In comparison, the ED2+ macrophages did not appear at the tendon-bone interface until eleven days after surgery. Our two-week time point may have missed the early decrease in ED1+ and the increase in ED2+ macrophages. We did not observe any migration of the ED1+ macrophages, again likely due to the relatively late observation time point of two weeks. Unlike the activity that was allowed in our study, animals in these previous studies were allowed ad libitum activity after surgery^{12,14}.

Bone formation also plays an important role in tendon-bone healing. This is the first study to use micro-CT to quantify bone volume and tissue mineral content at the bone-tendon interface in an ACL reconstruction model. We found that, compared with baseline values, the number of trabeculae was significantly lower after loading for four weeks, which partly supported our second hypothesis. These data agree with previous work showing that increased relative motion between the tendon graft and the bone tunnel in a rabbit model of ACL reconstruction was positively correlated with decreased bone ingrowth¹⁹. In that study, the areas with more motion and osteoclasts also had the slowest graft-to-tunnel healing time, suggesting that increased motion in the early postoperative stages may negatively impact tendon-bone healing. A previous rabbit model of ACL reconstruction also showed that inhibiting osteoclastic activity with osteoprotegerin improved bone formation at the tendon-bone interface as compared with that seen in animals that received RANKL to stimulate osteoclast activity²⁰. In contrast to the current study, that study found increased stiffness of the bone-graft-bone construct in the group with osteoclast inhibition, which may be due to the different levels of osteoclast stimulation and inhibition that were brought about by the pharmacological treatments.

Our final hypothesis was that immediate graft displacement would result in decreased strength and stiffness of the graft attachment. However, the load to failure of the isolated bone-graft-bone complex demonstrated no difference between immobilization and daily loading at both the two and four-week time points. Importantly, we did not compare with a group receiving normal cage activity. It is possible that both immobilization and immediate mechanical loading have adverse effects on graft healing and attachment strength as compared with the mechanical signals from "normal" activity.

It is also quite possible that differences would be seen at a later time point; we only evaluated animals for as long as four weeks in this preliminary study of our novel loading system.

In contrast to the results of this work, previous studies demonstrated the detrimental effect of stress deprivation on the biomechanical properties of tendons and ligaments²¹⁻²⁴. Our findings, however, are consistent with recent studies that examined tendon-to-bone healing in a rat rotator cuff model^{6,25}, in which, at eight weeks postoperatively, there was no change in structural properties according to activity level⁶. Interestingly, by the sixteen-week time point, immobilization positively affected structural properties as compared with the results seen with activity. This implies that eight to sixteen weeks of immobilization may be necessary to elicit biomechanical differences between graft-loading and immobilization. Comparison with our study may not be appropriate, however, since our study evaluated tendon-to-bone healing in a bone-tunnel model as opposed to tendon-healing to the bone surface and as there may have been differences in the magnitude of applied mechanical stimulus.

The loading that occurred just after the animal was killed, after removing all soft tissues except the graft, confirmed that the tendon graft was loaded according to our test protocol. However, a significant limitation of our model is that the load-displacement responses from the daily loading reflect the contributions of all soft tissues crossing the knee joint, not just the ACL graft. Although we sectioned all of the soft tissues crossing the joint (except for the posterior part of the capsule because of the risk of injury to posterior neurovascular structures), these tissues healed relatively rapidly in this small animal model. The isolated bone-tendon graft-bone construct shared 8% of the load across the joint at two weeks and 21% of the load across the joint at four weeks. Therefore, the *in vivo* loads required to achieve the target graft elongation at daily loading may reflect maturation of the tendon-graft interface and the graft itself, as well as healing of other soft tissues across the joint. Continued maturation of the healing tendon-bone interface over time, as demonstrated by increased ultimate load and stiffness, may be offset by weakening of the intra-articular segment of the graft and/or other soft tissues crossing the joint due to stress deprivation.

This investigation did not have any data available for an *a priori* power calculation. As a result, the study is likely to be underpowered, particularly with regard to the histological and micro-CT analyses. Despite this limitation, the results demonstrated some modest differences between immobilization and short-duration low-magnitude loading and provide a baseline for future studies to examine variables such as when to initiate the application of strain after surgery as well as the magnitude and duration of strain.

There are other limitations of this study. First, the baseline graft tension at the time of surgery could not be controlled in a quantifiable fashion. Second, the lack of biomechanical differences between immediate motion and immobilization may reflect the low level of applied graft strain. Furthermore, the duration of load application was less than fifteen minutes

per day, with the knee immobilized at all other times. Future studies should examine the effect of immediate motion with use of higher levels of applied strain, longer durations of loading, or more frequent loading sessions as well as the effect of delayed onset of loading after an initial period of immobilization. It is not known how our results might have differed if the animals had been allowed *ad libitum* activity. Finally, the applied motion in this study was limited to axial displacement of the graft, which differs from normal knee motion, which likely provides a complex loading environment on the tendon-bone construct during such activities. The conditions tested in this model do not directly reflect clinical practice but rather serve as an initial step in the study of the effect of load on tendon-to-bone healing in this novel model. We recognize that knee motion leads to a complex combination of tension, compression, and shear loads at the tendon-bone interface. Our goal was to isolate the loading environment to axial graft elongation, which could then be used as an independent study parameter.

In summary, this is the initial report of a new, *in vivo* model to evaluate tendon-healing in a bone tunnel. We found that low levels of mechanical stimulation for a short duration resulted in greater accumulation of ED1+ macrophages at the healing tendon-bone interface at two weeks following surgery and decreased trabecular number at the healing interface compared with baseline values. Within the parameters of loading studied herein, low levels of controlled loading starting in the immediate postoperative period do not significantly impair healing of the tendon-bone interface over the first four weeks following surgery. Future studies will assess the effect of variations in the timing, magnitude, and duration of controlled loading on tendon-bone healing after ACL reconstruction. ■

Robert H. Brophy, MD
Department of Orthopaedic Surgery,
Washington University School of Medicine,
14532 South Outer Forty Drive,
Chesterfield, MO 63017.
E-mail address: brophy@wudosis.wustl.edu

David Kovacevic, MD
Carl W. Imhauser, PhD
Mark Stasiak, MSE
Alice J.S. Fox, MD
Xiang-Hua Deng, MD
Scott A. Rodeo, MD
Hospital for Special Surgery, 535 East 70th Street,
New York, NY 10021

Asheesh Bedi, MD
Department of Orthopaedic Surgery,
University of Michigan,
1500 East Medical Center Drive,
2912 Taubman Center, Box 0328,
Ann Arbor, MI 48109-5328

References

1. Cooper RR, Misol S. Tendon and ligament insertion. A light and electron microscopic study. *J Bone Joint Surg Am.* 1970;52:1-20.
2. Rodeo SA, Arnoczky SP, Torzilli PA, Hidaka C, Warren RF. Tendon-healing in a bone tunnel. A biomechanical and histological study in the dog. *J Bone Joint Surg Am.* 1993;75:1795-803.
3. Whiston TB, Walmsley R. Some observations on the reactions of bone and tendon after tunnelling of bone and insertion of tendon. *J Bone Joint Surg Br.* 1960;42:377-86.
4. Grana WA, Egle DM, Mahnken R, Goodhart CW. An analysis of autograft fixation after anterior cruciate ligament reconstruction in a rabbit model. *Am J Sports Med.* 1994;22:344-51.
5. Panni AS, Milano G, Lucania L, Fabbriani C. Graft healing after anterior cruciate ligament reconstruction in rabbits. *Clin Orthop Relat Res.* 1997;343:203-12.
6. Thomopoulos S, Williams GR, Soslowsky LJ. Tendon to bone healing: differences in biomechanical, structural, and compositional properties due to a range of activity levels. *J Biomech Eng.* 2003;125:106-13.
7. Sakai H, Fukui N, Kawakami A, Kurosawa H. Biological fixation of the graft within bone after anterior cruciate ligament reconstruction in rabbits: effects of the duration of postoperative immobilization. *J Orthop Sci.* 2000;5:43-51.
8. Thomopoulos S, Zampiakos E, Das R, Silva MJ, Gelberman RH. The effect of muscle loading on flexor tendon-to-bone healing in a canine model. *J Orthop Res.* 2008;26:1611-7.
9. Beynnon BD, Johnson RJ, Fleming BC, Renström PA, Nichols CE, Pope MH, Haugh LD. The measurement of elongation of anterior cruciate-ligament grafts in vivo. *J Bone Joint Surg Am.* 1994;76:520-31.
10. Beynnon BD, Uh BS, Johnson RJ, Fleming BC, Renström PA, Nichols CE. The elongation behavior of the anterior cruciate ligament graft in vivo. A long-term follow-up study. *Am J Sports Med.* 2001;29:161-6.
11. Heijne A, Fleming BC, Renstrom PA, Peura GD, Beynnon BD, Werner S. Strain on the anterior cruciate ligament during closed kinetic chain exercises. *Med Sci Sports Exerc.* 2004;36:935-41.
12. Kawamura S, Ying L, Kim HJ, Dinybil C, Rodeo SA. Macrophages accumulate in the early phase of tendon-bone healing. *J Orthop Res.* 2005;23:1425-32.
13. Otsu N. A threshold selection method from gray-level histograms. *IEEE Trans.* 1979;SMC9:62-6.
14. Hays PL, Kawamura S, Deng XH, Dagher E, Mithoefer K, Ying L, Rodeo SA. The role of macrophages in early healing of a tendon graft in a bone tunnel. *J Bone Joint Surg Am.* 2008;90:565-79.
15. Marsolais D, Côté CH, Frenette J. Neutrophils and macrophages accumulate sequentially following Achilles tendon injury. *J Orthop Res.* 2001;19:1203-9.
16. McLennan IS. Resident macrophages (ED2- and ED3-positive) do not phagocytose degenerating rat skeletal muscle fibres. *Cell Tissue Res.* 1993;272:193-6.
17. Honda H, Kimura H, Rostami A. Demonstration and phenotypic characterization of resident macrophages in rat skeletal muscle. *Immunology.* 1990;70:272-7.
18. St Pierre BA, Tidball JG. Differential response of macrophage subpopulations to soleus muscle reloading after rat hindlimb suspension. *J Appl Physiol.* 1994;77:290-7.
19. Rodeo SA, Kawamura S, Kim HJ, Dinybil C, Ying L. Tendon healing in a bone tunnel differs at the tunnel entrance versus the tunnel exit: an effect of graft-tunnel motion? *Am J Sports Med.* 2006;34:1790-800.
20. Rodeo SA, Kawamura S, Ma CB, Deng XH, Sussman PS, Hays P, Ying L. The effect of osteoclastic activity on tendon-to-bone healing: an experimental study in rabbits. *J Bone Joint Surg Am.* 2007;89:2250-9.
21. Binkley JM, Peat M. The effects of immobilization on the ultrastructure and mechanical properties of the medial collateral ligament of rats. *Clin Orthop Relat Res.* 1986;203:301-8.
22. Hannafin JA, Arnoczky SP, Hoonjan A, Torzilli PA. Effect of stress deprivation and cyclic tensile loading on the material and morphologic properties of canine flexor digitorum profundus tendon: an in vitro study. *J Orthop Res.* 1995;13:907-4.
23. Noyes FR. Functional properties of knee ligaments and alterations induced by immobilization: a correlative biomechanical and histological study in primates. *Clin Orthop Relat Res.* 1977;123:210-42.
24. Woo SL, Gomez MA, Woo YK, Akeson WH. Mechanical properties of tendons and ligaments. II. The relationships of immobilization and exercise on tissue remodeling. *Biorheology.* 1982;19:397-408.
25. Gimbel JA, Van Kleunen JP, Williams GR, Thomopoulos S, Soslowsky LJ. Long durations of immobilization in the rat result in enhanced mechanical properties of the healing supraspinatus tendon insertion site. *J Biomech Eng.* 2007;129:400-4.